Biochemical characterization and mutational analysis of the mononuclear non-heme Fe2+ site in Dke1, a Cupin-type dioxygenase from Acinetobacter johnsonii

Stefan Leitgeb, Grit D Straganz, Bernd Nidetzky

Biochemical Journal Immediate Publication. Published on 30 Oct 2008 as manuscript BJ20081161

Biochemical characterization and mutational analysis of the mononuclear non-heme Fe^{2+} site in Dke1, a Cupin-type dioxygenase from *Acinetobacter johnsonii*

Stefan Leitgeb, Grit D. Straganz, and Bernd Nidetzky[1]

Institute of Biotechnology and Biochemical Engineering, Graz University of Technology, Petersgasse 12/1, A-8010 Graz, Austria

Running title: Mutational analysis of the mononuclear non-heme Fe^{2+} site of Dke1

Keywords: Non-heme iron; dioxygenase; cupin fold; metal site; mutational analysis

Abbreviations: Dke1, β-diketone-cleaving enzyme; CD, circular dichroism

[1] To whom correspondence should be addressed:

Bernd Nidetzky, Graz University of Technology, Institute of Biotechnology and Biochemical Engineering, Petersgasse 12, A-8010 Graz

Phone: +43 316 873 8400; Fax: +43 873 8434; E-mail: bernd.nidetzky@tugraz.at

Revised version BJ2008/1161

SYNOPSIS

β-Diketone-cleaving enzyme Dke1 is a homotetrameric Fe^{2+}-dependent dioxygenase from *Acinetobacter johnsonii.* The Dke1 protomer adopts a single-domain β-barrel fold characteristic of the Cupin superfamily of proteins and features a mononuclear non-heme Fe^{2+} centre where a triad of histidines, His-62, His-64, and His-104, coordinate the catalytic metal. To provide structure-function relationships for the peculiar metal site of Dke1 in relation to the more widespread 2-His-1-Glu/Asp binding site for non-heme Fe^{2+}, we replaced each histidine individually by Glu and Asn and compared binding of Fe^{2+} and four non-native, catalytically inactive metals to purified apo-forms of wild-type and mutant enzymes. Results from anaerobic equilibrium microdialysis (Fe^{2+}) and fluorescence titration (Fe^{2+}, Cu^{2+}, Ni^{2+}, Mn^{2+}, Zn^{2+}) experiments revealed the presence of two broadly specific metal binding sites in native Dke1 that bind Fe^{2+} with a dissociation constant (K_d) of 5 μM (site I) and ≈ 3 × 10^2 μM (site II). Each mutation except the substitution of His-104 by Asn disrupted binding of Fe^{2+}, but not that of the other divalent metal ions, at site I while leaving metal binding at site II largely unaffected. Dke1 mutants harbouring substitutions by Glu were completely inactive and not functionally complemented by external Fe^{2+}. The Fe^{2+} catalytic centre activity (k_{cat}) of mutants with Asn substitution of His-62 and His-104 was decreased 140- and 220-fold, respectively, as compared to the k_{cat} value of 8.5 s^{-1} for the wild-type enzyme in the reaction with 2,4-pentanedione. The His-64→Asn mutant was not catalytically competent, except in the presence of external Fe^{2+} (1 mM) which elicited about 1/1000 of wild-type activity. Therefore, coordination of Fe^{2+} by Dke1 requires an uncharged metallocentre, and 3 His ligands are needed for the assembly of a fully functional catalytic site. Oxidative inactivation of Dke1 was shown to involve conversion of enzyme-bound Fe^{2+} into Fe^{3+}, which is then released from the metal centre.

INTRODUCTION

Non-heme Fe^{2+} provides catalytic assistance to a variety of enzymatic reactions that utilize dioxygen as the co-substrate [1-5]. Contrasting their functional diversity in these O_2-dependent transformations, the protein metallo-centres that bind Fe^{2+} display a remarkably conserved structure. Typically, a facial triad of 2 histidines and 1 carboxylate residue, exemplified by the metallo-centres of a large class of 2-oxo-glutarate-dependent dioxygenases [6], form the primary coordination sphere for the Fe^{2+} cofactor [7, 8]. NMR-derived and crystal structures for several 2-His-1-Glu/Asp Fe^{2+} sites are now available and reveal a high degree of similarity in the spatial arrangement of the metal-coordinating side chains [8]. Interestingly, therefore, two lines of evidence suggest that the canonical 2-His-1-Glu/Asp centre is not at all selective for binding of Fe^{2+}. Firstly, *in vitro* experiments show that several divalent metals (e.g. Zn^{2+}, Cu^{2+}, Mn^{2+}) are strong competitive inhibitors of the binding of Fe^{2+}, their affinity for the metal site being similar to or even higher than that of the native Fe^{2+} [9]. Secondly, the 2-His-1-Glu/Asp centre is exploited by some extradiol-cleaving dioxygenases to coordinate Mn^{2+} as the catalytic metal [10]. Fe^{2+} inactivates these enzymes. It is not known what structural features of the protein determine the preference of one metal over the other [11].

Mutational analysis of the 2-His-1-Glu/Asp motif was carried out in different Fe^{2+} enzymes. Individual site-directed substitutions of the facial triad residues often resulted in a strong disruption of Fe^{2+} binding concomitant with loss of activity [12-15]. Notwithstanding these findings, definite answers to the question of how non-heme Fe^{2+} sites achieve their requisite metal binding selectivity remain elusive. The identification of novel Fe^{2+} centres featuring an alternate 3-His or 3-His-1-Glu pattern of Fe^{2+} coordination has recently rekindled the interest in relationships between

structure of non-heme Fe^{2+} sites and their function in metal binding and catalysis [16].

β-Diketone-cleaving enzyme Dke1 is a homotetrameric Fe^{2+}-dependent dioxygenase from *Acinetobacter johnsonii.* The enzyme catalyzes an unusual chemical reaction (EC 1.13.11.50) where molecular oxygen is used to convert 2,4-pentandione into methylglyoxal and acetate, as indicated in Scheme 1. Breakdown of the substrate occurs via the incorporation of one atom from molecular oxygen into each site of carbon-carbon bond fission. Studies of the reaction mechanism of Dke1 showed that the active-site Fe^{2+} is required in the formation of the enzyme-substrate complex and in dioxygen chemistry [17-19]. The x-ray crystal structure of an inactive form of Dke1 in which Fe^{2+} was replaced by adventitious Zn^{2+} (PDB-code: 3bal) reveals that the enzyme protomer adopts a single-domain β-barrel fold characteristic of the Cupin superfamily of proteins. It also leads to a suggestion for the mononuclear non-heme Fe^{2+} centre of the enzyme where a triad of histidines, His-62, His-64, and His-104, coordinate Fe^{2+} (Figure 1a). The putative ligands to the catalytic metal are contributed from two consensus regions in the Dke 1 primary structure which represent a conserved signature for Cupin-type metallo-proteins. A structure-based sequence comparison of Dke 1 with a representative series of non-heme metal enzymes (Figure 1b) shows that despite a very distant relatedness at the sequence level, the selected proteins have conserved the positions of the metal-coordinating residues. While His-62 and His-104 are invariant, the change of residue at Dke 1 position 64 determines the variable 2-His-1-Glu/Asp or 3-His pattern of the metal sites. In the crystal structure of halogenase SyrB2 in the resting state, halide is bound proximal to a non-coordinating Ala and seems to reconstitute the 2-His-1-carboxylate character of the Fe^{2+} centre [20]. Therefore, structural homology in a

range of non-heme metal centres is clearly reflected by residue conservation in the amino acid sequence.

The important and novel insight encapsulated by Figure 1b prompted us to analyze the putative non-heme Fe^{2+} centre of Dke 1 by site-directed mutagenesis, addressing the following questions in particular. Can we confirm the suggestion from the structure of the Zn^{2+} enzyme that the native Fe^{2+} cofactor is coordinated by three histidines? How does remodelling of the probable Fe^{2+} centre into one that features the alternate 2-His-1-Glu or 2-His-1-Asp pattern in the sequence affect the function of the active site with regard to metal binding and catalysis? The results portray a highly promiscous metal binding site of Dke 1 in which the natural 3-His pattern is a requirement not only for binding of Fe^{2+} but also for Fe^{2+}-dependent dioxygenase activity. They support the view that the 3-His Fe^{2+} site is not a mere peculiarity of the presently more widespread 2-His-1-Glu/Asp centre and should be regarded as an independent structural unit of Fe^{2+} enzyme function.

MATERIALS AND METHODS

Materials

If not otherwise stated, all chemicals were purchased from Sigma-Aldrich (Vienna, Austria) at the highest available purity. The metal salts used for binding studies were from Merck (Darmstadt, Germany). Enzymes for molecular cloning were obtained from MBI Fermentas (St. Leon-Rot, Germany) except *Pfu* DNA polymerase, which was from Promega (Madison, WI, USA). The plasmid expression vector pKYB1 was from New England Biolabs (Beverly, MA, USA).

Site-directed mutagenesis, gene expression, and protein purification

The method for generating site-directed mutants of Dke1 was based on a published two-stage PCR protocol [21]. The relevant mutagenic oligonucleotide primers are

summarized in Table S1 (see the Supporting Information). The vector pKYB1-*dke1-strep* [22] was used as the template. It is a variant of the commercial plasmid vector pKYB1 and encodes the wild-type form of Dke1 containing Strep-Tag II fused to the authentic C-terminal residue of the enzyme (Ala-153). DNA sequencing (MWG Biotech, Ebersberg, Germany) of all mutagenized constructs was used to verify that only the desired substitutions had been introduced. Gene expression in *E. coli* BL21 (DE3) and purification of the mutants was done exactly as in prior work [22]. We used fresh or very carefully regenerated column material in the isolation of wild-type and mutated enzymes, essentially ruling out any cross-contamination of the protein preparations used. Also note that the *E. coli* strain does not contain a Dke1 homologue which despite the high selectivity of the affinity interaction exploited in the purification might be carried over into the isolated proteins. Purified protein preparations were brought to a concentration of about 5 mg/mL in 20 mM Tris-HCl, pH 7.5, and stored at – 20 °C until further use. Each Dke1 mutant migrated in SDS PAGE as a single protein band that showed the expected molecular mass of about 18 kDa for the full-length protein including the tag (data not shown). Molar protein concentrations were determined as described previously [17], using a value of 1.9 g/L for the molar extinction coefficient of the Dke1 subunit at 280 nm. If not mentioned otherwise, all experiments were performed in 20 mM Tris-HCl buffer, pH 7.5.

Protein-bound iron, and kinetic measurement of its release into solution

We used a photometric assay with FereneS [23, 24], which forms a stable coloured complex with Fe^{2+} ($\varepsilon_{592\ nm}$ = 35.5 $mM^{-1}\ cm^{-1}$). The reagent was added in excess (10 mM) to the diluted enzyme preparation (20 – 60 µM protein subunit), from which unbound iron had been detached via 3 cycles of buffer exchange using NAP columns from GE Healthcare (Chalfont St. Giles, UK). Determination of the total amount of

protein-bound iron requires that any Fe^{3+} present be reduced to Fe^{2+}. Therefore, an ascorbic acid concentrate (20 mM) was adjusted to pH 6.0 with NaOH and added to an end concentration of 2 mM in the cuvette. The total volume of the assay was 1000 µL. The cuvette was incubated in the temperature-controlled cell holder of a Beckmann Coulter DU 800 UV/VIS spectrophotometer, and the change in absorbance at 592 nm was monitored continuously over time until after 6 to 8 hours, the absorption remained constant. From the obtained end-point absorbance after substraction of the blank, the molar iron content was calculated.

A similar assay was used to determine the rate of dissociation of the metal cofactor from Dke1. Twenty µL of enzyme solution (~ 500 µM Fe^{2+}-containing protomer) was mixed with 980 µL of a solution of 20 mM Ferene S in 20 mM Tris-HCl buffer, pH 7.5, and the increase in absorbance at 592 nm was measured continuously for ≈ 2 min in the spectrophotometer. It was observed that formation of the complex between Ferene S and Fe^{2+} was not rate-determining under these conditions, implying that the measured metal release rates were kinetically unmasked. The Ferene S solution used was equilibrated with a mixture of N_2 and O_2 to give concentrations of dissolved dioxygen between 50 and 800 µM. The actual concentration of O_2 in the assay was measured immediately before and after the reaction using a fiber optic microsensor (Microtox TX3-AOT; PreSens, Regensburg, Germany). It was found that start and end concentration of O_2 differed not more than 20%, and the mean value of the two measurements was used for evaluation of data. To distinguish between the release of Fe^{2+} and that of total iron (= Fe^{2+} + Fe^{3+}) under the different O_2 conditions, we repeated each assay in the presence of 2 mM sodium ascorbate. It was found in control experiments that chemical reduction of Fe^{3+} by ascorbate in solution was more than 10 times faster than the dissociation of protein-bound Fe^{2+}. The rate of Fe^{3+} appearance (V_{Fe3+}) was calculated from the difference in

the rates of formation of total iron and dissociation of Fe^{2+}. V_{Fe3+} is kinetically complex as it describes the overall process of oxidation of Fe^{2+} at the catalytic site of Dke1 and the release of Fe^{3+} into solution.

Reversible metal exchange in wild-type and mutant forms of Dke1, and its effect on activity

The Fe^{2+} bound to purified preparations of wild-type Dke1 or site-directed mutants thereof was exhaustively removed by dialysis using Slide-A-Lyzer Dialysis cassettes from Pierce Biotechnology Inc. (Rockford IL, USA). Concentrated enzyme solutions (~ 1mM) were dialyzed against 2 mM EDTA in 20 mM Tris-HCl buffer, pH 7.5, at 4°C over night. Afterwards buffer was exchanged with 20 mM Tris-HCl, pH 7.5, and dialyzed 2 times for 8-12 hours at 4°C. Quantitative stripping of iron from the enzyme was controlled by activity measurements with 2,4-pentanedione and iron quantification using the FereneS assay. The apo-enzymes thus obtained were incubated on ice for 30 to 60 minutes in the presence of 2 mM metal ion (Fe^{2+}, Zn^{2+}, Ni^{2+}, Cu^{2+}, or Mn^{2+}) that was added as the sulphate salt. When Fe^{2+} was used, 2 mM sodium ascorbate was also added to prevent Fe^{2+} oxidation. Unbound metal ion was removed by 3 cycles of gel filtration using the NAP columns described above, and the resulting preparations were used for enzyme activity measurements.

Enzyme activity assays

O_2-dependent activity of Dke1 towards 2,4-pentanedione (200 µM) was determined either spectrophotometrically by measuring substrate depletion at 280 nm ($\varepsilon_{280\ nm}$ = 2.2 $mM^{-1}\ cm^{-1}$) [17] or with an oxygen electrode cell (Digital Oxygen System model 10, Rank Brothers, Cambridge, UK) measuring oxygen consumption dependent on substrate cleavage. Reactions were performed in a total volume of 600 µL in air-saturated (260 µM oxygen) 20 mM Tris-HCl buffer at pH 7.5 and 25°C. One unit is defined as the conversion of 1 µmol substrate per minute. Alternative reactivities

towards 330 μM of substrates quercetin, potassium oxalate and 3,4-dihydroxyphenylacetate were investigated in the oxygen electrode cell. Reactions were carried out in the presence of 650 μM $MnCl_2$ (potassium oxalate; 3,4-dihydroxyphenylacetate) or $CuSO_4$ (quercetin). All traces recorded with the oxygen electrode cell were corrected for a blank rate lacking enzyme.

Inactivation of Dke1

About 200 μM of Fe^{2+}-containing active sites of Dke1 were incubated at 25 °C in an air-saturated buffer to which one of different metal ions (Fe^{2+}, Fe^{3+}, Zn^{2+}, Ni^{2+}, Cu^{2+}, or Mn^{2+}) had been added in 1.2 to 10-fold molar excess over metal binding centres. Be aware the ferric iron was added as citrate complex the other metal ions as sulphate. A sample (5 μL) was taken from the mixture (0.2 mL) every 10 to 30 min, and 1 μL of it was diluted immediately into the spectrophometric assay for Dke1 activity. It was observed that the concentration of metal ion introduced to the assay with the sample did not interfere with the activity measurement.

Equilibrium microdialysis

Experiments were performed in an anaerobic glove box from Plas-Labs (Lansing, MI, USA). The concentration of O_2 in all solutions was smaller than 2 μM. Microdialysis buttons were from Hampton Research (Aliso Viejo CA, USA) with a chamber volume of 25 μL. The protein concentrations used were in the range 140 – 435 μM. Dialysis was performed against 25 mL of 20 mM Tris-HCl buffer, pH 7.5, with $FeSO_4$ added to a final concentration of between 0.01 and 2.00 mM. A membrane with a molecular weight cut-off of 12,000 – 14,000 was used. Control experiments showed that there was no protein leakage through the membrane and binding of protein and ligand to the chamber walls of the microdialysis button and the membrane was negligible. The dialysis was carried out for up to 5 hours at 25 °C, and it was found that this was long

enough to attain the binding equilibrium. The concentration of free Fe^{2+} was determined using the assay with Ferene S.

Data was processed using Scatchard analysis (Equation 1),

$$\frac{[L]_b}{[L]_f [E]_t} = -\frac{1}{K_d}\frac{[L]_b}{[E]_t} + \frac{n}{K_d} \qquad \text{(Eq. 1)}$$

where $[L]_b$ and $[L]_f$ are the bound and free ligand concentrations, respectively, and $[E]_t$ is the total concentration of ligand binding sites, n is the number of independent binding sites, and K_d is the dissociation constant. The data were visualized in plots of $[L]_b/([L]_f\,[E]_t)$ against $[L]_b/[E]_t$ which according to Equation 1 should be linear with a slope of $\tilde{1}/K_d$.

Fluorescence titration experiments

We used fluorescence titration analysis to determine the binding of different metal ions to apo-enzymes of wild-type Dke1 or site-directed mutants thereof. The change of intrinsic protein fluorescence served as indirect reporter of the binding event [9]. Fluorescence data was collected at 4 °C using a Hitachi F-4500 Fluorescence Spectrophotometer. Titration experiments were performed using 0.3 – 2.3 µM enzyme dissolved in a 20 mM Tris-HCl buffer, pH 7.5, that had been made anaerobic in the glove box ($[O_2]$ < 2 µM). The used quartz cuvettes were sealed with a septum to avoid diffusion of air oxygen into the solution. Metal was added in portions of 1 - 20 µL from a concentrated stock solution of the respective chloride or sulphate salt to give a concentration in the cuvette ranging from 0.005 to 2.00 mM. It was shown by comparing results obtained with $ZnCl_2$ and $ZnSO_4$ that the used anion did not affect the results of fluorescence titration. At each metal concentration, a full emission wavelength scan was performed. The excitation wavelength was 290 nm, and

emission scans were recorded between 300 and 400 nm. Signal intensity was measured at the respective wavelength of maximal fluorescence which varied in dependence of the enzyme or the metal ion used between 328 and 340 nm. Within a series, the same emission wavelength was used for all data points. Excitation and emission slit widths were both 5.0 nm, and the photomultiplier voltage was set to 950 V. Spectra were recorded with a scan speed of 1200 nm/min in fivefold repetition, averaged and smoothed using the software package FL solutions delivered with the fluorescence spectrophotometer.

Data was fitted with the appropriate equation using nonlinear regression analysis with SigmaPlot 9.0. Equation 2 describes ligand binding to a single (tightly binding) protein site, where *y* is the change, typically the quenching of fluorescence intensity, and *a* is the maximum value of *y* at saturating total ligand concentration $[L]_t$. Equation 3 describes ligand binding to two independent protein sites that differ in binding affinity, where $K_{d,1}$ and $K_{d,2}$ are dissociation constants for sites I and II, and *a* and *b* are the maximum changes of *y* resulting from saturation of sites I and II with ligand, respectively.

$$y = \frac{a\left([E]_t + [L]_t + K_d\right) - \sqrt{\left([E]_t + [L]_t + K_d\right)^2 - 4[E]_t[L]_t}}{2[E]_t} \qquad \text{(Eq. 2)}$$

$$y = \frac{a\left([E]_t + [L]_t + K_{d,1}\right) - \sqrt{\left([E]_t + [L]_t + K_{d,1}\right)^2 - 4[E]_t[L]_t}}{2[E]_t} + \frac{b[L]_t}{K_{d,2} + [L]_t} \qquad \text{(Eq. 3)}$$

Enzymatic conversion of 2,4-pentanedione analyzed by HPLC

Reactions were carried out in a total volume of 0.6 mL using air-saturated 20 mM sodium citrate buffer, pH 7.5, that contained 5 mM 2,4-pentanedione as the substrate. One mM Fe^{2+} and 2 mM sodium ascorbate were also added to the reaction mixtures. The enzyme concentration was ≈ 100 μM for the mutant enzymes

and 25 nM for wild-type Dke1. After start of the reaction by adding the enzyme, incubation was continued at 25 °C for about 4.5 h. Samples were taken every 30 minutes, centrifuged and subsequently analyzed by HPLC with a Merck-Hitachi La Chrom system (Darmstadt, Germany) equipped with an Aminex HPX-87H column (Biorad, Hercules, CA, USA) as well as UV and RI detectors. Elution was performed with sulphuric acid (0.005 M) at a flow rate of 0.6 mL/min and a column temperature of 65 °C was used.

RESULTS

Structural properties of metal site mutants of Dke1

Purified site-directed mutants of Dke1 were analyzed by CD spectroscopy. The wild-type enzyme in the native Fe^{2+}-bound form as well as in the inactive apo-form were also analyzed and used as reference. The distribution of secondary structure elements derived from the CD spectra was in very reasonable agreement with the crystal structure of Dke 1. Point mutation of the metal-coordinating histidines did not alter the content of secondary structural elements as compared to the wild-type (Table S2). Like the wild-type enzyme, all mutants eluted as tetramers in gel filtration analysis (data not shown).

Wild-type Dke1 contained about 0.9 mol equivalents of Fe^{2+} bound to each protein subunit. With the exception of the H104E and H104N variants that displayed a fractional saturation with Fe^{2+} of 0.27 and 0.45, respectively, all other Dke1 mutants as isolated contained less than 5% bound Fe^{2+} (see Table S2). Mutants harbouring substitution of His by Glu or Asp as well as the H62N and H64N enzymes did not show activity in initial rate assays where in the presence of 2,4-pentandione the consumption of dicarbonyl substrate or O_2 co-substrate was measured. By contrast,

the H104N mutant displayed about 1% of the specific activity (0.09 U/mg) of the wild-type enzyme.

Binding of Fe^{2+} determined by equilibrium microdialysis

Data was acquired for wild-type Dke1 and three point mutants thereof in which His-64 had been replaced by Asp, Glu or Asn. For each enzyme, a Scatchard plot was constructed from measurements of the concentration of free Fe^{2+} in a series of binding equilibria resulting from the variation of the initial concentration of the ligand. The results are summarized in Figure 2. The Scatchard plot for Fe^{2+} binding by the apo-form of the wild-type enzyme was curved and showed two regions at low and high concentration of bound metal where the relationship between $r/[L]_f$ and r was linear. r is the number of bound Fe^{2+} molecules per protein molecule. The results in Figure 2 suggest that the protomer of wild-type Dke1 possesses 2 nonequivalent metal binding sites, which differ in their affinity for Fe^{2+}. The Scatchard plot indicates one binding site with high affinity and either one or two additional sites with lower affinity for Fe^{2+}. Plots of the fractional occupancy of the enzyme with metal ion as a function of the logarithmic ligand concentration (data not shown) also reveal the biphasic nature of the binding event. From the slopes of the straight lines fitted to the data at low and high values of r (see Figure 2), rough estimates for the dissociation constants (K_d) of the binding site with high (site I) and low affinity (site II) were obtained, considering that according to eqn. (1) the slope of the Scatchard plot equals K_d. These K_d values differ by at least an order of magnitude and are confirmed by results of fluorescence titration experiments to be described later. Concentrations of Fe^{2+} (≤ 100 μM) well below the K_d for site II restored native levels of dioxygenase activity in apo Dke1, suggesting that Fe^{2+} site I represents the catalytic centre. Characterization of site II was not further pursued since it is not thought to be important catalysis due to its low affinity for Fe^{2+}.

Figure 2 also shows that the biphasic characteristic of Fe^{2+} binding by the wild-type enzyme was completely disrupted in all three His-64 mutants of Dke1. Straight-line fits of the data for each mutant in Figure 2 yielded K_d estimates that were identical within limits of error (30 %) to the K_d value for Fe^{2+} binding to site II in the wild-type enzyme. The cross-section of the best line fit with the x-axes also reveals the presence of only 1 independent Fe^{2+} binding site.

Metal binding to wild-type and mutant forms of Dke1 determined by fluorescence titration

In addition to Fe^{2+}, we selected a series of four divalent metal ions (Cu, Mn, Ni, Zn) that occur naturally in Cupin-type metallo-proteins [25-28]. Change in the intensity of intrinsic tryptophan fluorescence upon addition of ligand to the anaerobic protein solution was used as reporter of metal binding to Dke1 or site-directed mutants thereof. Except for binding of Zn^{2+} to H104E and H104N that was characterized by an enhancement of fluorescence intensity, all other binding events were accompanied by quenching of the fluorescence signal of between 10 – 40 % (Mn^{2+}, Ni^{2+}, Zn^{2+}) and up to 100% (Fe^{2+}, Cu^{2+}) of its value in the unliganded protein. Fluorescence titration data for binding of Fe^{2+} to the wild-type enzyme is displayed in Figure 3a. Saturatable binding at high ligand concentration was observed for all of enzyme-metal combinations studied, suggesting that a possible nonspecific component to total ligand binding was small under the conditions used. The isotherms for binding of Fe^{2+} (Figure 3a) and Cu^{2+} (data not shown) by the wild-type enzyme were biphasic, as expected for a protein that has multiple nonequivalent binding sites for the ligand. By contrast, the corresponding binding isotherms for the Dke1 mutants with ferrous iron were simple hyperbolas, consistent with a situation where the protein has only a single binding site or multiple equivalent binding sites for the ligand. The H104N enzyme was an exception as titration data indicated two independent binding sites

for Fe^{2+} (Figure 3b). Equation 3 was used to fit biphasic binding events whereas Equation 2 was used to fit simple Langmuir isotherms. Results are summarized in Table 1.

The calculated K_d values for binding of Fe^{2+}, Cu^{2+}, Mn^{2+}, Ni^{2+}, and Zn^{2+} to wild-type Dke1 were very similar. They were therefore assigned to metal binding at site I ($K_{d,1}$). These results provide an explanation for the presence of adventitious metal (e.g. Zn^{2+}) in several preparations of Dke1 [17] including the one for which the x-ray structure has been solved. Site-directed replacements used to substitute His-62, His-64, or His-104 destroyed completely - with the notable exception of the H104N enzyme - the binding of Fe^{2+} at site I whereas they had comparably small effects on binding of the other metals. Only in the H62N mutant did we observe a clear disruption in the apparent binding of Cu^{2+}, Mn^{2+}, and Ni^{2+}, as compared to the binding of these metals to the wild-type enzyme. The H104N enzyme was the only Dke1 variant that retained binding affinity for Fe^{2+} at site I. The comparably high Fe^{2+} content of the H104N mutant as isolated is fully consistent with this observation. It was difficult to obtain a precise value for $K_{d,1}$ from the binding isotherm (Figure 3b) and only a rough estimate of ≤ 1 μM can be given. Binding of Fe^{2+} seems to be tighter in the H104N enzyme than in wild-type Dke1. It is important to note that the mutations did not affect binding of Fe^{2+} and Cu^{2+} to the low-affinity site II of Dke1, represented by the value of $K_{d,2}$. The values of $K_{d,1}$ for binding of Fe^{2+} and $K_{d,2}$ for binding of Fe^{2+} and Cu^{2+} agree reasonably with K_d estimates obtained in microdialysis experiments.

Reversible inactivation of Dke1 by external metal ions

An immediate suggestion of the results of Table 1 is that Cu^{2+}, Mn^{2+}, Ni^{2+}, and Zn^{2+} will promote reversible inactivation of wild-type Dke1 through their competition with the native Fe^{2+} cofactor for binding to the metal centre. When a solution of 200 μM

Fe^{2+}-containing active sites of Dke1 was incubated at 25 °C in the presence of a 1.2-fold molar excess of one of the divalent metals mentioned above, loss of enzyme activity as a function of time was accelerated, by a factor of up to 10, as compared to a control that did not contain external metal (Note: It was for practical reasons not possible to exclude O_2 in the stability experiments. The oxidation of Fe^{2+} in solution may therefore constitute a relevant component of the basal inactivation rate of Dke1 in the absence of added metal.) Plots of the natural logarithm of the residual enzyme activity against incubation time were linear until about 80 % of the initial activity had been lost (data not shown). The slopes of these plots are summarized in Table 2 for a comparison of the kinetic stability of the enzyme under the different conditions used, however, without implying that inactivation of Dke1 can be generally analyzed as a pseudo-first order process. Fe^{3+} (added as a metal citrate complex) had no effect on the inactivation rate of the enzyme whereas a 10-fold molar excess of Fe^{2+} over Dke1 active sites in the presence of 2 mM sodium ascorbate resulted in a significant, ≈ 2-fold stabilization.

The rate constant of Fe^{2+} detachment from Dke1 (k_{diss}) was determined in the presence of 20 mM Ferene S and had a value of about 0.04 min^{-1}. It was ensured by using a 1000-fold molar excess of metal-chelating reagent that trapping of the released Fe^{2+} was both quantitative and fast enough to be not kinetically significant under the conditions used. k_{diss} approximates the rate constant of enzyme inactivation at low protein concentration (0.05 μM), where binding of Fe^{2+} to Dke1 is not a relevant factor. The relative effectiveness of external metals in speeding up the inactivation of Dke1 thus seems to reflect their relative binding rates to the apo-form of the enzyme. “Fast binders” such as Cu^{2+}, Ni^{2+} or Co^{2+} hence promote activity loss in Dke1 at rates comparable to that seen in the presence of Ferene S.

We examined restoration of Dke1 activity resulting from the displacement of enzyme-bound Zn^{2+} by external Fe^{2+}. A 10-fold molar excess of Fe^{2+} (2 mM; + 2 mM sodium ascorbate) was added to a Dke1 preparation that had lost > 90% of the original activity after incubation in the presence of Zn^{2+}. About 30% of the specific activity measured prior to the inactivation was recovered during the time of the assay (5 min), clearly demonstrating that binding of catalytically incompetent metals is a reversible process.

Analysis of the mechanism of oxidative inactivation of wild-type Dke1

Incubation of Dke1 (≈ 1000 μM Fe^{2+}-containing active sites) at 25 °C in the presence of a molar equivalent of H_2O_2 (20 mM Tris-HCl buffer, pH 7.5) caused complete loss of enzyme activity in less than 10 min. A gel-filtered preparation of thus inactivated Dke1 did not contain bound Fe^{2+}, but had retained the tetrameric structure of the native enzyme. Addition of 2 mM Fe^{2+} to it caused partial (≈ 40%) reconstitution of the original specific activity. These results demonstrate that Dke1 is highly susceptible to oxidative denaturation. They also show that the overall process of enzyme inactivation by H_2O_2 is reversible, at least partly. We speculated that reversible inactivation involves oxidation of protein-bound Fe^{2+} followed by release of Fe^{3+} into solution.

The proposed denaturation of Dke1 was examined using O_2 as the oxidant. O_2 rather than H_2O_2 was chosen considering that auto-inactivation of the enzyme by the co-substrate of the catalytic reaction would be a process of potential physiological relevance. We employed an initial-rate assay that measured in the presence of Ferene S (20 mM) the velocity of appearance of Fe^{2+} in solution under conditions in which sodium ascorbate was lacking or added in a concentration of 2 mM. Ferric ion released from the enzyme escapes detection in this assay unless it is reduced to Fe^{2+} by ascorbate. Because all of the free ferrous ion is effectively trapped in the

complex with Ferene S, secondary oxidation of Fe^{2+} in solution is negligible under the used experimental settings. Figure 4 summarizes results obtained at different concentrations of dissolved O_2. Dissociation of Fe^{2+} occurred with a frequency of about 2×10^{-2} min^{-1} that was independent on the O_2 concentration used. By contrast, the rate of total iron loss, determined in the presence of ascorbate, was significantly enhanced by increased levels of O_2, indicating that O_2 promotes loss of cofactor from the active site as Fe^{3+} as shown in Figure 4. A straight-line fit of the data yielded a second-order rate constant of 0.09 M^{-1} min^{-1} for the O_2 dependence of this process, in which oxidation of Fe^{2+} and release of Fe^{3+} from the enzyme are steps of potential kinetic significance. Rate measurements for the appearance of total iron, that is Fe^{2+} and Fe^{3+}, agreed very well with the rates of loss of enzyme activity for dilute Dke1 preparations recorded under otherwise identical conditions, indicating that the reported data is internally consistent.

Effect of structural changes at the metallo-centre of Dke1 on enzymatic catalysis to O_2-dependent reactions

The Dke1 mutants were assayed for activity under initial rate conditions where a minimum concentration of 0.7 µM Fe^{2+}-containing active sites was used and consumption of 2,4-pentanedione was measured spectrophotometrically. They were all inactive below a detection limit of 0.01 % of the catalytic centre activity (k_{cat}) of 8.5 s^{-1} for wild-type Dke1 [17], except the H62N and H104N enzymes that displayed k_{cat} values of 4 (± 1) $\times 10^{-2}$ s^{-1} and 6.0 (± 1.3) $\times 10^{-2}$ s^{-1}, respectively.

We attempted functional complementation of the otherwise inactive mutants of Dke1 through the addition of external Fe^{2+} (1 mM; + 2 mM sodium ascorbate). Initial rate assays based on on-line measurement of O_2 consumption or spectrophotometric detection of conversion of 2,4-pentandione are not compatible with this amount of soluble Fe^{2+}. We therefore determined by HPLC the time courses of formation of

acetate and methylglyoxal from 2,4-pentandione (5 mM) catalyzed by wild-type (0.025 μM) and mutant (100 μM) forms of Dke1. Reactions lacking Fe^{2+} or the enzyme were used as controls. Like the controls, H62E, H64D, H64E, and H104E enzymes did not show detectable activity. By contrast, the H64N mutant promoted conversion of the substrate in a manner that was strictly dependent on external Fe^{2+}. From the linear plot of 2,4-pentandione used against the reaction time (≤ 5 h; data not shown) an apparent catalytic centre activity of 2.8 (± 0.7) × 10^{-3} s^{-1} was calculated. It can be compared with a k_{cat} of 2.15 (± 0.05) s^{-1} for the wild-type enzyme measured under the same reaction conditions containing free Fe^{2+} and ascorbate.

Hybrid enzymes generated by substituting the native Fe^{2+} in wild-type Dke1 by Cu^{2+}, Mn^{2+} or Ni^{2+} were completely inactive towards O_2 (260 μM) when one of the following substrates was offered to a protein solution containing 100 μM metal sites: 2,4-pentanedione (200 μM); quercetin (330 μM); potassium oxalate (330 μM); 3,4-dihydroxyphenylacetate (330 μM). None of the mutant enzymes displayed detectable activity under otherwise identical reaction conditions.

DISCUSSION

The 3-His centre of non-heme Fe^{2+} constitutes a conserved structural motif in an increasing number of oxygenase active sites [29]. Its evolution in the Cupin superfamily of proteins alongside the well known 2-His-1-Asp/Glu motif raises the interesting, yet unanswered question of how variations in primary coordination sphere contribute to fine tuning of metal binding selectivity and chemical reactivity in natural non-heme Fe^{2+} sites. To our knowledge, this work on Dke1 is the first study that delineates structure-function relationships for a 3-His Fe^{2+} centre through detailed comparison of the wild-type enzyme and relevant site-directed mutants thereof.

Mutational analysis of the 3-His metallocentre of Dke1

Site-directed mutants of Dke1 in which His-62, His-64 or His-104 had been replaced by a Glu lost all (H62E, H64E) or most (H104E) of the affinity of the wild-type dioxygenase for binding of Fe^{2+} at the catalytic site and were completely inactive in assays measuring O_2-dependent conversion of 2,4-pentanedione. Because the mutants were properly folded and could bind divalent metals other than Fe^{2+} almost as well as the wild-type enzyme did (see the discussion below), we conclude that the metallocentre of Dke1 was not globally disrupted as result of the site-directed substitutions. The functional defect resulting from the mutations was not complemented by external Fe^{2+}, suggesting that it was not just on the affinity for the metal cofactor but also on catalysis. The absence of detectable activity in the H104E mutant, which was isolated with a fractional Fe^{2+} occupancy of ≈ 0.3, supports this notion. These results strongly reinforce the proposal from the x-ray structure of a Zn^{2+}-bound form of wild-type Dke1 that His-62, His-64, and His-104 are ligands to the catalytic Fe^{2+} in the native enzyme.

Substitution of His-64 by Glu or Asp mimics in Dke1 the characteristic sequence pattern for Fe^{2+} coordination via the facial triad 2-His-1-Glu/Asp (Figure 1b). However, like in the H64E mutant, the His-64→Asp replacement was not compatible with binding of Fe^{2+} at the active site and dioxygenase activity towards 2,4-pentanedione. We therefore mutated His-64 into Asn to avoid the increase in overall negative net charge of the metal centre that is expected to result at neutral pH from the replacement of an uncharged His side chain by the anionic side chain of Asp or Glu. While the isolated H64N enzyme displayed a similar defect in Fe^{2+} binding as the other His-64 mutants, it differed from H64E and H64D in that the addition of external Fe^{2+} could elicit ≈ 0.1% wild-type level of Dke1 activity in its otherwise inactive apo-form.

H62N and H104N mutants of Dke1 were therefore examined and found to have retained about 0.5% of wild-type catalytic activity in the absence of external Fe^{2+}. The H104N enzyme appeared to have even gained Fe^{2+} binding affinity as compared to the native enzyme. The aggregate data thus reveals the retention of a catalytic Fe^{2+} centre in the His→Asn mutants of Dke1. Moreover it strongly supports the notion that binding of Fe^{2+} and catalysis to O_2-dependent carbon-carbon bond cleavage in 2,4-pentanedione by Dke1 requires a non-heme metal site that maintains an overall neutral charge, as in the native 3-His and mutated 2-His-1-Asn forms of the enzyme. However, the Asn residue, especially that at position 104, substitutes the corresponding native His better during Fe^{2+} binding than in catalysis.

The 2-His-1-Glu/Asp centres for non-heme Fe^{2+} in the Cupin-type oxygenases 1-aminocyclopropane-1-carboxylase, isopenicillin N synthase, prolyl 4-hydroxylase, and taurine dioxygenase have been probed with site-directed mutagenesis, substituting each of the ligands to Fe^{2+} by an alternatively coordinating amino acid or the non-coordinating Ala [12, 13, 15, 30-32]. From a comparison of reported data for residual iron content and activity in isolated mutants of these enzymes one gets a general picture fully consistent with our findings for metal site mutants of Dke1 that the defect in catalysis to O_2 chemistry is usually greater than that in Fe^{2+} binding (reviewed in [33]). Replacements by Asn of Asp-414 in prolyl 4-hydroxylase [30] and Asp-179 in 1-aminocyclopropane-1-carboxylase [15] yield the same putative 2-His-1-Asn centre for Fe^{2+} as it is proposed here for the H64N mutant of Dke1. The D414N and D179N mutants were inactive, notably in spite of the presence of 50 μM Fe^{2+} in the activity assay for the prolyl 4-hydroxylase.

Metal binding selectivity and catalysis to O_2 chemistry

Ligand binding data obtained in equilibrium microdialysis and fluorescence titration experiments independently support the existence of two nonequivalent Fe^{2+} binding

sites in Dke1. Competitive binding studies in which reversible inactivation of Dke1 in the presence of incompetent metal ions was examined allowed unequivocal assignment of the high-affinity Fe^{2+} site to the catalytic centre of the enzyme. The low-affinity binding site showed unmistakable interactions with Fe^{2+} and Cu^{2+}. Because its location in the structure of Dke1 is not defined and the fractional occupancy with metal ligand will normally be negligible considering $K_{d,2}$ values in the range 50 – 320 μM, analysis of this binding site was not further pursued.

In fluorescence titration experiments the 3-His metal centre of Dke1 did not show detectable affinity to a complex of Fe^{3+} and citrate (data not shown). Considering that upon oxidation of the Fe^{2+} cofactor the resulting Fe^{3+} is rapidly released into solution, we therefore propose the metal centre of Dke1 distinguishes clearly between Fe^{2+} and the oxidized Fe^{3+}. Differential binding recognition of ferrous and ferric forms of iron has so far not been reported for the 3-His centre. The catalytic Fe^{2+} site of Dke1 is highly promiscous concerning the binding of divalent metal ions other than iron. It shares this unusual property with quercetin dioxygenase that has a 3-His-1-Glu metal centre [34]. However, unlike Dke1, various metals (Co^{2+}, Cu^{2+}, Ni^{2+}, Mn^{2+}, Fe^{3+}) are capable of eliciting activity in quercetin dioxygenase (from *Bacillus subtilis*) [34, 35].

With a K_d of about 5 μM, binding of Fe^{2+} to Dke1 is barely stronger than binding of Cu^{2+}, Mn^{2+}, Ni^{2+} and Zn^{2+}. Kinetic hindrance to the release of Fe^{2+} from the native holo-enzyme ($k_{diss} \approx 2 \times 10^{-2}$ min^{-1}; see Table 2) could be a mechanism through which Dke1 delays inactivation resulting from a thermodynamically driven exchange of metals at its active site. Individual mutagenesis of the Fe^{2+} coordinating His-62, His-64, and His-104 by Glu and Asn and furthermore His-64 by Asp caused a highly selective disruption of metal binding recognition, affecting exclusively the Fe^{2+} among the series of metal ions tested. The substitution His-62→Asn was an

exception as it resulted in a globally weakened binding of divalent metals. Despite being recognized by wild-type and mutated metal sites of Dke1, the non-native metal ions did not elicit enzyme activity during a screening for relevant substrate transformations catalyzed by Cupin-type oxygenases, that is, quercetin dioxygenase [34]; oxalate oxidase [36] or homoprotocatechuate 2,3-dioxygenase [37]. The native Fe^{2+} enzyme was likewise inactive in reactions other than C-C bond cleavage in 2,4-pentanedione.

Reactions at the metallo-centre that lead to inactivation of Dke1

Isolated Dke1 is not stable in solution at ambient temperature. Scheme 2 summarizes pathways of reversible inactivation of the enzyme that involve decomposition of the functional non-heme Fe^{2+} centre. A decrease in fractional Fe^{2+} occupancy below a level expected from the value of K_d under given reaction conditions is promoted by secondary oxidation of the released Fe^{2+} and competitive binding of other divalent metals to the active site. The Fe^{2+} bound in the active site is protected markedly against oxidation by dissolved O_2 as compared to the Fe^{2+} in solution. However, at high O_2 levels and probably in a H_2O_2 environment it becomes a main contributor to the observed inactivation rate. The oxidative inactivation is a two-step process that involves first the rate-determining formation and then the comparably fast release of Fe^{3+}.

Summarizing, we present for the first time a detailed biochemical characterization and mutational analysis of a 3-His centre for mononuclear non-heme Fe^{2+}. The results for Dke1 suggest that alongside the well known 2-His-1-Glu/Asp centre, the 3-His site has evolved as an independent structural and functional unit in Cupin-type oxygenases, thereby broadening the landscape for Fe^{2+}-dependent catalysis in a diverse superfamily of β-barrel metalloproteins. The conclusion is

reinforced by recent evidence from biomimetic chemistry, showing that a trispyrazolylborato iron malonato complex (where Fe^{2+} is coordinated by 3 N donor ligands) serves as a functional small-molecule model of the active site of Dke1 in the O_2-dependent cleavage of β-diketones [38].

REFERENCES

1 Myers, R. W., Wray, J. W., Fish, S. and Abeles, R. H. (1993) Purification and characterization of an enzyme involved in oxidative carbon-carbon bond cleavage reactions in the methionine salvage pathway of *Klebsiella pneumoniae*. J. Biol. Chem. **268**, 24785-24791

2 Roach, P. L., Clifton, I. J., Fulop, V., Harlos, K., Barton, G. J., Hajdu, J., Andersson, I., Schofield, C. J. and Baldwin, J. E. (1995) Crystal structure of isopenicillin N synthase is the first from a new structural family of enzymes. Nature. **375**, 700-704

3 Vaillancourt, F. H., Yin, J. and Walsh, C. T. (2005) SyrB2 in syringomycin E biosynthesis is a nonheme FeII α-ketoglutarate- and O_2-dependent halogenase. Proc. Natl. Acad. Sci. U S A. **102**, 10111-10116

4 Joseph, C. A. and Maroney, M. J. (2007) Cysteine dioxygenase: structure and mechanism. Chem. Commun., 3338-3349

5 Earhart, C. A., Vetting, M. W., Gosu, R., Michaud-Soret, I., Que, L., Jr. and Ohlendorf, D. H. (2005) Structure of catechol 1,2-dioxygenase from *Pseudomonas arvilla*. Biochem. Biophys. Res. Commun. **338**, 198-205

6 Purpero, V. and Moran, G. R. (2007) The diverse and pervasive chemistries of the α -keto acid dependent enzymes. J. Biol. Inorg. Chem. **12**, 587-601

7 Hegg, E. L. and Que, L., Jr. (1997) The 2-His-1-carboxylate facial triad - an emerging structural motif in mononuclear non-heme iron(II) enzymes. Eur. J. Biochem. **250**, 625-629

8 Clifton, I. J., McDonough, M. A., Ehrismann, D., Kershaw, N. J., Granatino, N. and Schofield, C. J. (2006) Structural studies on 2-oxoglutarate oxygenases and related double-stranded beta-helix fold proteins. J. Inorg. Biochem. **100**, 644-669

9 Dunning Hotopp, J. C., Auchtung, T. A., Hogan, D. A. and Hausinger, R. P. (2003) Intrinsic tryptophan fluorescence as a probe of metal and α -ketoglutarate binding to TfdA, a mononuclear non-heme iron dioxygenase. J. Inorg. Biochem. **93**, 66-70

10 Whiting, A. K., Boldt, Y. R., Hendrich, M. P., Wackett, L. P. and Que, L., Jr. (1996) Manganese(II)-dependent extradiol-cleaving catechol dioxygenase from *Arthrobacter globiformis* CM-2. Biochemistry. **35**, 160-170

11 Boldt, Y. R., Whiting, A. K., Wagner, M. L., Sadowsky, M. J., Que, L., Jr. and Wackett, L. P. (1997) Manganese(II) active site mutants of 3,4-dihydroxyphenylacetate 2,3-dioxygenase from *Arthrobacter globiformis* strain CM-2. Biochemistry. **36**, 2147-2153

12 Grzyska, P. K., Muller, T. A., Campbell, M. G. and Hausinger, R. P. (2007) Metal ligand substitution and evidence for quinone formation in taurine/α-ketoglutarate dioxygenase. J. Inorg. Biochem. **101**, 797-808

13 Kreisberg-Zakarin, R., Borovok, I., Yanko, M., Frolow, F., Aharonowitz, Y. and Cohen, G. (2000) Structure-function studies of the non-heme iron active site of isopenicillin N synthase: some implications for catalysis. Biophys. Chem. **86**, 109-118

14 Li, M., Muller, T. A., Fraser, B. A. and Hausinger, R. P. (2008) Characterization of active site variants of xanthine hydroxylase from *Aspergillus nidulans*. Arch. Biochem. Biophys. **470**, 44-53

15 Zhang, Z., Barlow, J. N., Baldwin, J. E. and Schofield, C. J. (1997) Metal-catalyzed oxidation and mutagenesis studies on the iron(II) binding site of 1-aminocyclopropane-1-carboxylate oxidase. Biochemistry. **36**, 15999-16007

16 Straganz, G. D. and Nidetzky, B. (2006) Variations of the 2-His-1-carboxylate theme in mononuclear non-heme Fe(II) oxygenases. ChemBioChem. **7**, 1536-1548

17 Straganz, G. D., Glieder, A., Brecker, L., Ribbons, D. W. and Steiner, W. (2003) Acetylacetone-cleaving enzyme Dke1: a novel C-C-bond-cleaving enzyme from *Acinetobacter johnsonii*. Biochem. J. **369**, 573-581

18 Straganz, G. D., Hofer, H., Steiner, W. and Nidetzky, B. (2004) Electronic substituent effects on the cleavage specificity of a non-heme Fe^{2+}-dependent β-diketone dioxygenase and their mechanistic implications. J. Am. Chem. Soc. **126**, 12202-12203

19 Straganz, G. D. and Nidetzky, B. (2005) Reaction coordinate analysis for β-diketone cleavage by the non-heme Fe^{2+}-dependent dioxygenase Dke1. J. Am. Chem. Soc. **127**, 12306-12314

20 Blasiak, L. C., Vaillancourt, F. H., Walsh, C. T. and Drennan, C. L. (2006) Crystal structure of the non-haem iron halogenase SyrB2 in syringomycin biosynthesis. Nature. **440**, 368-371

21 Wang, W. and Malcolm, B. A. (1999) Two-stage PCR protocol allowing introduction of multiple mutations, deletions and insertions using QuikChange Site-Directed Mutagenesis. Biotechniques. **26**, 680-682

22 Straganz, G. D., Slavica, A., Hofer, H., Mandl, U., Steiner, W. and Nidetzky, B. (2005) Integrated approach for production of recombinant acetylacetone dioxygenase from *Acinetobacter johnsonii*. Biocatal. Biotransform. **23**, 261-269

23 Higgins, T. (1981) Novel chromogen for serum iron determinations. Clin. Chem. **27**, 1619-1620

24 Johnson-Winters, K., Purpero, V. M., Kavana, M., Nelson, T. and Moran, G. R. (2003) (4-Hydroxyphenyl)pyruvate dioxygenase from *Streptomyces avermitilis*: the basis for ordered substrate addition. Biochemistry. **42**, 2072-2080

25 Cleasby, A., Wonacott, A., Skarzynski, T., Hubbard, R. E., Davies, G. J., Proudfoot, A. E., Bernard, A. R., Payton, M. A. and Wells, T. N. (1996) The x-ray crystal structure of phosphomannose isomerase from *Candida albicans* at 1.7 Å resolution. Nat. Struct. Biol. **3**, 470-479

26 Pochapsky, T. C., Pochapsky, S. S., Ju, T., Mo, H., Al-Mjeni, F. and Maroney, M. J. (2002) Modeling and experiment yields the structure of acireductone dioxygenase from *Klebsiella pneumoniae*. Nat. Struct. Biol. **9**, 966-972

27 Woo, E. J., Dunwell, J. M., Goodenough, P. W., Marvier, A. C. and Pickersgill, R. W. (2000) Germin is a manganese containing homohexamer with oxalate oxidase and superoxide dismutase activities. Nat. Struct. Biol. **7**, 1036-1040

28 Fusetti, F., Schroter, K. H., Steiner, R. A., van Noort, P. I., Pijning, T., Rozeboom, H. J., Kalk, K. H., Egmond, M. R. and Dijkstra, B. W. (2002) Crystal structure of the copper-containing quercetin 2,3-dioxygenase from *Aspergillus japonicus*. Structure. **10**, 259-268

29 Dunwell, J. M., Purvis, A. and Khuri, S. (2004) Cupins: the most functionally diverse protein superfamily? Phytochemistry. **65**, 7-17

30 Myllyharju, J. and Kivirikko, K. I. (1997) Characterization of the iron- and 2-oxoglutarate-binding sites of human prolyl 4-hydroxylase. Embo J. **16**, 1173-1180

31 Doan, L. X., Hassan, A., Lipscomb, S. J., Dhanda, A., Zhang, Z. and Schofield, C. J. (2000) Mutagenesis studies on the iron binding ligands of clavaminic acid synthase. Biochem. Biophys. Res. Commun. **279**, 240-244

32 Sinnecker, S., Svensen, N., Barr, E. W., Ye, S., Bollinger, J. M., Jr., Neese, F. and Krebs, C. (2007) Spectroscopic and computational evaluation of the structure of the high-spin Fe(IV)-oxo intermediates in taurine: alpha-ketoglutarate dioxygenase from *Escherichia coli* and its His99Ala ligand variant. J. Am. Chem. Soc. **129**, 6168-6179

33 Leitgeb, S. and Nidetzky, B. (2008) Structural and functional comparison of 2-His-1-Carboxylate and 3-His metallocentres in non-heme iron(II) dependent enzymes Biochem Soc Trans, in press

34 Gopal, B., Madan, L. L., Betz, S. F. and Kossiakoff, A. A. (2005) The crystal structure of a quercetin 2,3-dioxygenase from *Bacillus subtilis* suggests modulation of enzyme activity by a change in the metal ion at the active site(s). Biochemistry. **44**, 193-201

35 Schaab, M. R., Barney, B. M. and Francisco, W. A. (2006) Kinetic and spectroscopic studies on the quercetin 2,3-dioxygenase from *Bacillus subtilis*. Biochemistry. **45**, 1009-1016

36 Opaleye, O., Rose, R. S., Whittaker, M. M., Woo, E. J., Whittaker, J. W. and Pickersgill, R. W. (2006) Structural and spectroscopic studies shed light on the mechanism of oxalate oxidase. J. Biol. Chem. **281**, 6428-6433

37 Vetting, M. W., Wackett, L. P., Que, L., Jr., Lipscomb, J. D. and Ohlendorf, D. H. (2004) Crystallographic comparison of manganese- and iron-dependent homoprotocatechuate 2,3-dioxygenases. J. Bacteriol. **186**, 1945-1958

38 Siewert, I. and Limberg, C. (2008) A trispyrazolylborato iron Malonato complex as a functional model for the acetylacetone dioxygenase. Angew. Chem. Int. Ed. Engl. **47**, 7953-7956

39 DeLano, W. L. (2002) The PyMOL Molecular Graphics System. In., DeLano Scientific, Palo Alto, CA, USA

40 Stranzl, G. R. (2002) X-ray crystal structure of acetylacetone-cleaving dioxygenase of *Acinetobacter johnsonii* and NMR evidence for a strong short hydrogen bond in the active site of HbHNL. PhD-Thesis. *Institute of Chemistry*, Karl Franzens University Graz, Graz, Austria

41 Simmons, C. R., Liu, Q., Huang, Q., Hao, Q., Begley, T. P., Karplus, P. A. and Stipanuk, M. H. (2006) Crystal structure of mammalian cysteine dioxygenase. A novel mononuclear iron center for cysteine thiol oxidation. J. Biol. Chem. **281**, 18723-18733

42 Pochapsky, T. C., Pochapsky, S. S., Ju, T., Hoefler, C. and Liang, J. (2006) A refined model for the structure of acireductone dioxygenase from *Klebsiella* ATCC 8724 incorporating residual dipolar couplings. J. Biomol. NMR. **34**, 117-127

43 Roach, P. L., Clifton, I. J., Hensgens, C. M., Shibata, N., Schofield, C. J., Hajdu, J. and Baldwin, J. E. (1997) Structure of isopenicillin N synthase complexed with substrate and the mechanism of penicillin formation. Nature. **387**, 827-830

44 Zhang, Z., Ren, J.-S., Clifton, I. J. and Schofield, C. J. (2004) Crystal structure and mechanistic implications of 1-aminocyclopropane-1-carboxylic acid oxidase - the ethylene-forming enzyme. Chem. Biol. **11**, 1383-1394

45 Elkins, J. M., Ryle, M. J., Clifton, I. J., Dunning Hotopp, J. C., Lloyd, J. S., Burzlaff, N. I., Baldwin, J. E., Hausinger, R. P. and Roach, P. L. (2002) X-ray crystal structure of *Escherichia coli* taurine/α-ketoglutarate dioxygenase complexed to ferrous iron and substrates. Biochemistry. **41**, 5185-5192

46 Zhang, Z., Ren, J., Stammers, D. K., Baldwin, J. E., Harlos, K. and Schofield, C. J. (2000) Structural origins of the selectivity of the trifunctional oxygenase clavaminic acid synthase. Nat. Struct. Biol. **7**, 127-133

FIGURE LEGENDS

Figure 1. The 3-His metal centre in a zinc-bound structure of Dke1 (panel a), and structure-based partial sequence alignment of non-heme metal dependent enzymes (panel b). The figure in panel A was generated with PyMOL 0.99 [39]. In panel B, the conserved histidine residues (His-62 and His-104 in Dke1) are shown in yellow. The variable metal ligand (His-64 in Dke1) is shown in green. Numbers indicate the length of the intermotif region separating the conserved motifs shown. Dke1 = diketone dioxygenase from *Acinetobacter johnsonii* [40], CDO = cysteine dioxygenase from *Rattus norvegicus* [41], SyrB2 = halogenase SyrB2 from *Pseudomonas syringae* pv. *syringae* B301D [20], ARD = acireductone dioxygenase from *Klebsiella ATCC 8724* [42], IPNS = isopenicillin N synthase from *Aspergillus nidulans* [43], CAA = carbonic anhydrase from *Homo sapiens* (pdb ID 1IF4), ACCO = 1-Aminocyclopropane-1-carboxylic acid oxidase from *Petunia hybrida* [44], TauD = taurine dioxygenase from *Escherichia coli* [45], CAS = Clavaminate synthase from *Streptomyces clavuligerus* [46].

Figure 2. Scatchard plot of equilibrium microdialysis data for wild-type Dke1 and site-directed mutants thereof. Cross sections of the line of best fit with the x-axis indicate the number of independent binding sites. ● and solid line, wild type, high affinity binding site; • and long dashed line, wild type, low affinity binding site; □ and dotted line, H64E; ▼ and short dashed line, H64D; Δ and dashed and dotted line, H64N. $[L]_b$ and $[L]_f$ are the concentrations of bound and free ligand (Fe^{2+}), respectively. $[E]_t$ is the total concentration of Dke1 metal binding sites.

Figure 3. Fluorescence titration data showing binding of Fe^{2+} to wild-type and H104N forms of Dke 1.

(a) Wild-type enzyme; data was collected with an enzyme concentration of 0.5 μM. (b) H104N; data was collected with an enzyme concentration of 0.9 μM. $K_{d,1}$ was fixed to 1 μM (see text for details). Solid lines show non-linear fits of the data using Equation 3.

Figure 4. Oxidative inactivation of Dke1 monitored as the rate of release of iron cofactor. The rates of dissociation of Fe^{2+} (o) and total iron (•) were measured. Note that due to the presence of ascorbic acid, the highest achievable O_2 concentration was about 0.8 mM.

Scheme 1: Proposed mechanism of O_2-dependent conversion of 2,4-pentanedione at the non-heme Fe^{2+} site of Dke1.

Scheme 2: Mechanisms causing inactivation of Dke1 (E) in the presence of O_2.

TABLES

Table 1. Dissociation constants for various metal complexes of wild-type and mutated forms of Dke1. K_d values are in μM and were obtained from non-linear fits of Equation 2 (single binding site) or Equation 3 (two binding sites) to fluorescence titration data. Data is organized in an upper and lower row to indicate metal binding to the high and low affinity metal binding site of the enzymes, respectively. n.a., not applicable; n.d. not determinded. Unless otherwise indicated, K_d values have S.D. of < 25%. [a] S.D. < 50 %; [b] S.D. < 66 %, [c] S.D. < 83 %.

	Fe^{2+}	Cu^{2+}	Mn^{2+}	Ni^{2+}	Zn^{2+}
Wild-type	5.2 [b] ~ 320	3.1 [a] ~ 600	5.5 n.a.	4.7 [a] n.a.	4.0 n.a.
H62E	n.a. ~ 150	6.3 [a] ~ 500	23 [a] n.a.	15 [a] n.a.	7.3 n.a.
H62N	n.a. ~ 50	n.a. ~ 80	33 [a] n.a.	29 [a] n.a.	n.d.
H64D	n.a. ~ 50	10 [c] ~ 600	6.1 [b] n.a.	10 [a] n.a.	12 [b] n.a.
H64E	n.a. ~ 100	32 ~ 500	12 n.a.	23 [a] n.a.	7.8 n.a.
H64N	n.a. ~ 70	28 ~ 1000	19 n.a.	9.6 n.a.	4.3 [a] n.a.
H104E	n.a. ~ 40	2.5 ~ 300	14 [a] n.a.	42 [b] n.a.	3.2 [a] n.a.
H104N	≤ 1 ~ 200	1.2 ~ 160	9.9 [a] n.a.	2.8 [a] n.a.	4.8 [b] n.a.

Table 2. External metals promote inactivation of Dke1. Apparent first-order rate constants of inactivation are shown. The concentrations of enzyme and metal were 200 μM and 240 μM, respectively. [a] Rate constant of Fe^{2+} detachment from the enzyme (200 μM) measured in the presence of 20 mM Ferene S. [b] Measured at a protein concentration of 0.05 μM. [c] Measured in the presence of 2 mM Fe^{2+} and 2 mM sodium ascorbate.

Additive	k [$10^{-2} \times min^{-1}$]
	0.19
-	(4.0)[a]
	(2.0)[b]
Fe^{2+} + ascorbate [c]	0.10
Fe^{3+}	0.18
Mn^{2+}	0.53
Co^{2+}	1.8
Ni^{2+}	2.2
Cu^{2+}	2.2
Zn^{2+}	0.46
Mg^{2+}	0.47

Figure 1

(a)

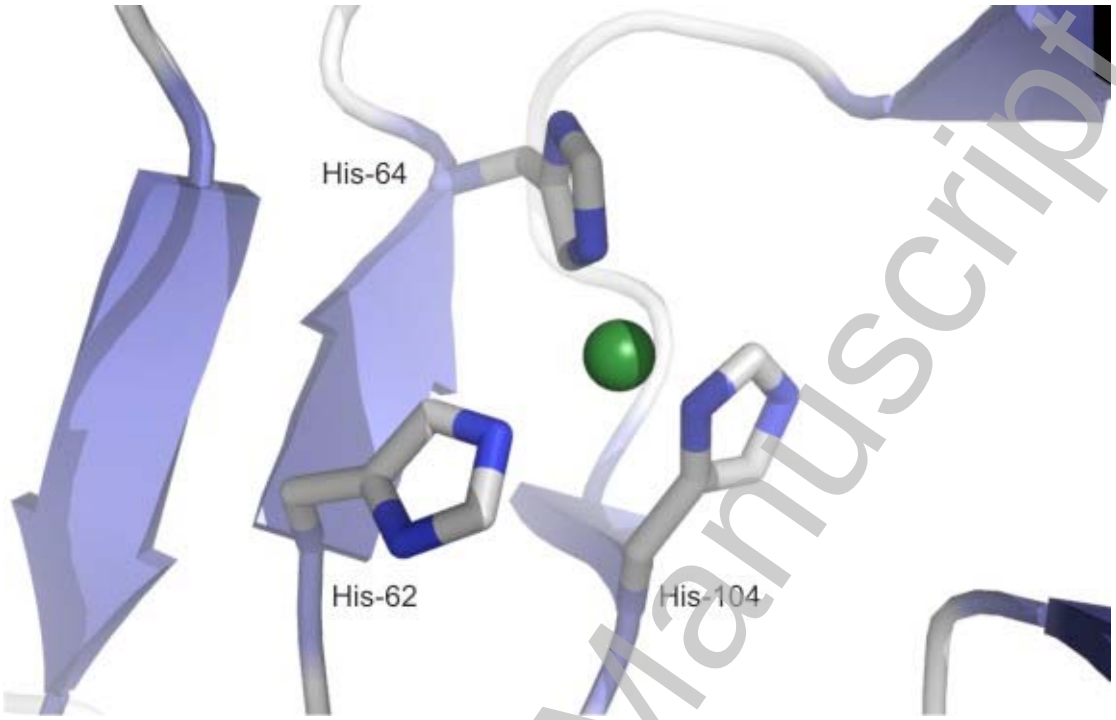

(b)

Dke1	GSSFASHIHAGPGEY	27	ESSGALHGKTFFP
CDO	GHGSSIHDHTDSHCF	40	NDSIGLHRVENVS
SyrB2	DEGTDWHQADTFANA	105	FWSTLMHASYPHS
ARD	EKFLNEHTHGE~DEV	31	VPAHTPHWFDMGS
IPNS	KLSFEWHEDVSLITV	42	YYKAPIHRVKWVN
CAA	YRLIQFHFHWGSLDG	11	KYAAELHLVHWNT
ACCO	IKGLRAHTDAGGIIL	43	KYKSVMHRVIAQK
TauD	PDNDNWHTDVTFIET	142	DNRVTQHYANADY
CAS	ETLLEFHTEMAYHRL	121	DNFRTTHARTPFS

Figure 2

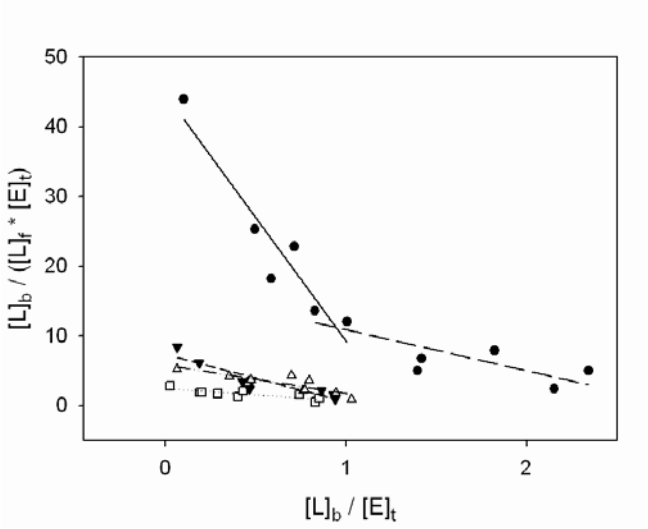

Figure 3

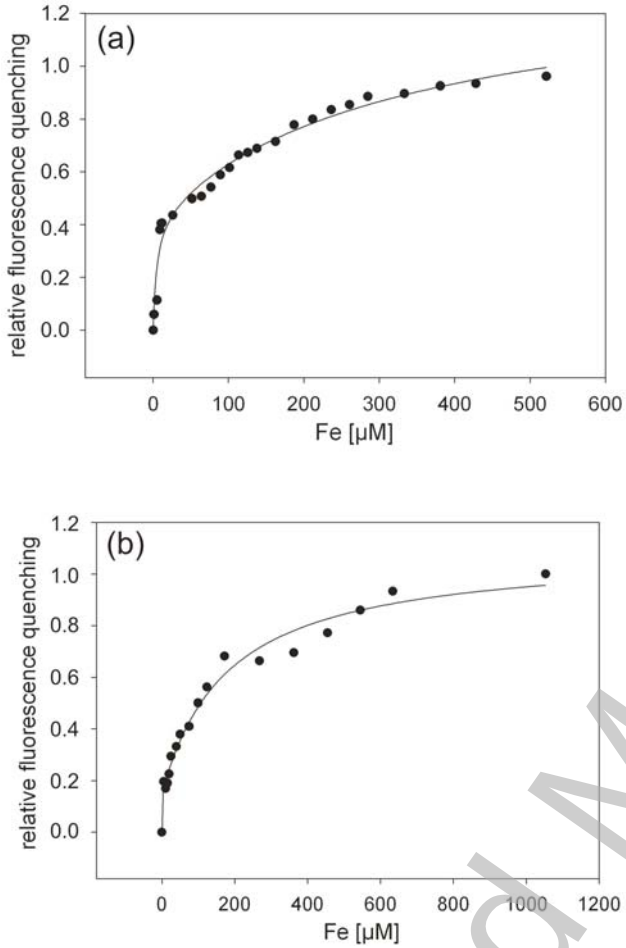

Figure 4

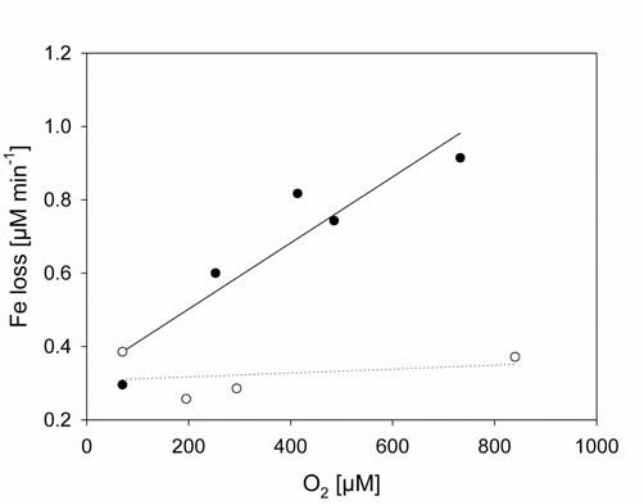

Scheme 1:

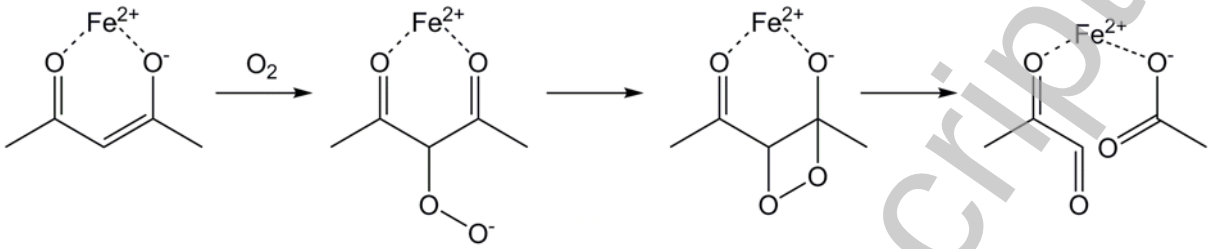

Scheme 2: